Journal of Organometallic Chemistry 695 (2010) 1012–1018

Contents lists available at ScienceDirect

Journal of Organometallic Chemistry

journal homepage: www.elsevier.com/locate/jorganchem

Crown ether complexes of tin(II) trifluoromethanesulfonate

Rajoshree Bandyopadhyay, Benjamin F.T. Cooper, Aaron J. Rossini, Robert W. Schurko, Charles L.B. Macdonald *

Department of Chemistry and Biochemistry, University of Windsor, Windsor, Ontario, Canada N9B 3P4

ARTICLE INFO

Article history:
Received 30 September 2009
Received in revised form 18 December 2009
Accepted 23 December 2009
Available online 4 January 2010

Keywords:
Main group
Tin
Low valent
Crown ether
Coordination chemistry

ABSTRACT

The treatment of tin(II) trifluoromethanesulfonate with three differently-sized crown ethers [12]crown-4, [15]crown-5 and [18]crown-6 results in the formation of tin complexes that exhibit dramatically different structural features. The compounds are investigated using experimental techniques and density functional theory calculations.

1. Introduction

The phenomenal ligand properties of the family of macrocyclic polyethers known as crown ethers have been used since the late 1960s in order to isolate numerous remarkable complexes for elements from throughout the periodic table [1]. In spite of the often interesting nature of the compounds obtained using elements from the s- and d-blocks, the crown ether chemistry of the p-block elements has not been examined nearly as extensively [2]. Recently, we found that differently-sized crown ethers allow for the ready isolation of Ge^{II} cations, including dications that do not feature any covalent bonds to the semi-metal center; [3–5] these results complement the observations of systems with the related cryptand ligands [6] and suggest that the use of such macrocyclic ligands should provide for a rich and interesting chemistry for even more of the p-block elements. In fact, we had previously found that crown ether ligation of our indium(I) trifluoromethanesulfonate (triflate) reagent $In^{I}O_3SCF_3$ ($In^{I}OTf$) [7] allows for the isolation of stable and isolable monomeric indium(I) complexes that exhibit unusual and perhaps useful modes of reactivity including oxidative addition into aliphatic carbon–chlorine bonds [8–11].

In light of the isovalent or isoelectronic relationship of Sn^{II} with Ge^{II} and In^{I}, respectively, and as part of our continuing investigation of the chemistry of crown ether complexes of p-block elements in low oxidation or valence states [12], we were interested in examining the crown ether chemistry of tin(II) analogues. It should be noted that Nicholson and co-workers prepared crystalline crown ether complexes of Sn^{II} halides in the 1980s as part of investigations about the nature of stereochemically-active "lone pairs" of electrons [13,14], some of which had been investigated spectroscopically prior to elucidation of their structural features [15,16], and the [18]crown-6 macrocycle was employed recently by Feldmann and co-workers to prepare an interesting mixed-valent tin iodide salt [17]. It should also be emphasized that our investigations of In^{I} and Ge^{II}, in conjunction with other well-known behavior, demonstrate that there are sometimes significant difference between the chemistry of main group element halides and the corresponding triflate analogues in terms of both relative stability and the structures of the complexes that may be isolated. Given the foregoing, in the present work, we detail the results of experimental and computational studies of tin(II) triflate with crown ethers of three different sizes.

2. Results and discussion

2.1. Experimental investigations

The treatment of equimolar amounts of [18]crown-6 with $Sn^{II}OTf_2$ in toluene or THF results in the formation of a colorless solution that provides upon concentration crystalline material in excellent yield characterized by microanalysis, multinuclear NMR spectroscopy and single crystal X-ray diffraction as [Sn([18]-crown-6)OTf][OTf], **1**[OTf]. The salt **1**[OTf] crystallizes in the space group $P\bar{1}$ with one formula unit in the asymmetric unit, which is illustrated in Fig. 1. The structure of the salt is best-described as

* Corresponding author. Tel.: +1 5199737098.
E-mail address: cmacd@uwindsor.ca (C.L.B. Macdonald).

0022-328X/$ - see front matter © 2009 Elsevier B.V. All rights reserved.
doi:10.1016/j.jorganchem.2009.12.023

consisting of a mono-cationic fragment composed of the crowned tin(II) center, which appears to be bound to one of the triflate groups, and a separate triflate anion. The covalent radii of Sn and O are 1.40 Å and 0.73 Å, respectively and the ionic radii for Sn(+2) and O(−2) are 0.93 Å and 1.40 Å, respectively [18]. It thus appear as if only the Sn–O bond to the closest triflate anion, at a distance of 2.282(9) Å, could possibly be treated as a "normal" single bond. The shortest Sn–O distance for the other triflate fragment is 2.596(9) Å, which falls within the sum of the van der Waals radii for Sn (2.19 Å) and O (1.52 Å), but is far longer than a typical single bond. For comparative purposes, it should be noted that the Sn^{II}–OTf distances in the Cambridge Structural Database (CSD) [19] range from 2.253–3.074 Å (average: 2.544 Å) however the longer distances reported are certainly best described as being for mostly ionic interactions. Furthermore, although the estimated standard deviations (esd) are relatively large, the various S–O distances in **1**[OTf] are also consistent with description above of the two different types of triflate fragments: the "bound" triflate fragment exhibits the two short S–O bonds and one long S–O bond anticipated for a more covalent triflate, whereas the "free" triflate has smaller range of S–O distances consistent with an isolated anion.

Overall, the salt-like composition of the complex more closely resembles the structure we observed for [Ge([15]crown-5)OTf][OTf] rather than the more symmetrical structure adopted for the [18]crown-6 complex of $Ge^{II}OTf_2$, as one might expect in light of the different sizes of Sn^{II} and Ge^{II} [3]. In terms of tin(II) chemistry, the structure of **1**[OTf] is clearly related to the halide complexes reported by Nicholson of the form [Cl-Sn([18]crown-6)][A] (A = $SnCl_3$ and ClO_4) in that it contains a mono-cationic Sn^{II} fragment in which the substituent bonded to the tin atom lies nearly normal to the crown ether. In the case of the chlorinated cation, the face opposite the substituent does not feature unusually-close contacts and appears to suggest the presence of a stereochemically-active "lone pair" of electrons and the results of Mössbauer spectroscopy suggest that this is perhaps a reasonable description, although the data suggest that the "lone pair" has a very high 5s character [13]. However, in the case of **1**[OTf], the relatively close distance of the second triflate renders the situation somewhat more ambiguous; the nature of cation is examined in more detail below using computational methods.

In spite of the structural features observed in the solid state, the ^{19}F NMR spectrum of **1**[OTf] in CD_2Cl_2 solution features only a single peak (even at 238 K) and could thus be consistent either with the complete dissociation of the salt into $[Sn([18]crown-6)]^{+2}$ and two anionic triflate ions or, perhaps more likely, the rapid exchange of the free and bound triflate groups on the NMR timescale. It should be noted that the salt does not exhibit any observable resonance in the ^{119}Sn NMR in solution but features a signal with an isotropic chemical shift at −1578 ppm in the solid state. None of the other NMR spectra exhibit any features that are worthy of note.

In light of the similarity of the cationic fragment **1** with In([18]-crown-6), and the previous results of Nicholson [14], we reasoned that the smaller [15]crown-5 should likely produce a "crown sandwich" and thus the reaction was undertaken using a 2:1 ratio of crown ether to tin. The reaction in THF proceeded as anticipated and generated $[Sn([15]crown\text{-}5)_2][OTf]_2$, **2**$[OTf]_2$, in virtually quantitative yield upon removal of the volatile components, however the material often contained impurities (either residual solvent or crown ether). Recrystallization of the material from CH_2Cl_2 produced crystalline material that was generally of poor quality in terms of its suitability for analysis by single crystal X-ray diffraction. Several samples were twinned and disordered significantly and, although they confirmed the proposed connectivity, they provided extremely low-quality solutions. The solution for the highest quality data set we obtained is illustrated in Fig. 2. Again, the data were of poor quality but were adequate to confirm that the structure does, in fact, contain an unambiguously dicationic "crown sandwich" of Sn^{II} that does not appear to bear a stereochemically-active pair of non-bonding electrons. Given the low-quality of the data, the values obtained for the metrical parameters are not suitable for extensive discussion but they are consistent with those reported by Nicholson and co-workers for $[Sn([15]crown\text{-}5)_2][SnCl_3]_2$ [14].

As in the case of **1**[OTf], the ^{119}Sn NMR spectrum of the salt in solution does not feature any observable resonances but the

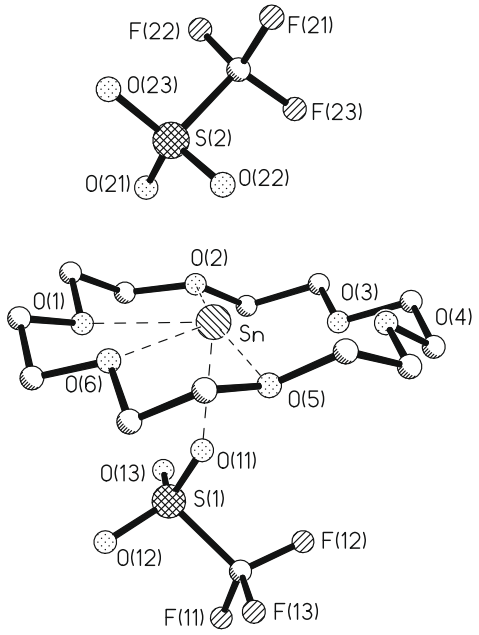

Fig. 1. Solid state structure of [Sn([18]crown-6)OTf][OTf], **1**[OTf] – hydrogen atoms are omitted for clarity. Selected metrical parameters including distances (Å) and angles (°): Sn–O(11), 2.282(9); Sn–O(21), 2.596(9); Sn–O(1), 2.506(6); Sn–O(2), 2.767(5); Sn–O(3), 3.026(6); Sn–O(4), 3.013(6); Sn–O(5), 2.712(6); Sn–O(6), 2.464(6); S(1)–O(11), 1.449(9); S(1)–O(12), 1.409(8); S(1)–O(13), 1.416(7); S(2)–O(21), 1.437(9); S(2)–O(22), 1.432(7); S(2)–O(23), 1.414(8); O(11)–Sn–O(21), 148.7(3); plane(O(1)–O(6))∠Sn–O(11), 7.6(2) (where a value of 0 would indicate that the bond is normal to the plane).

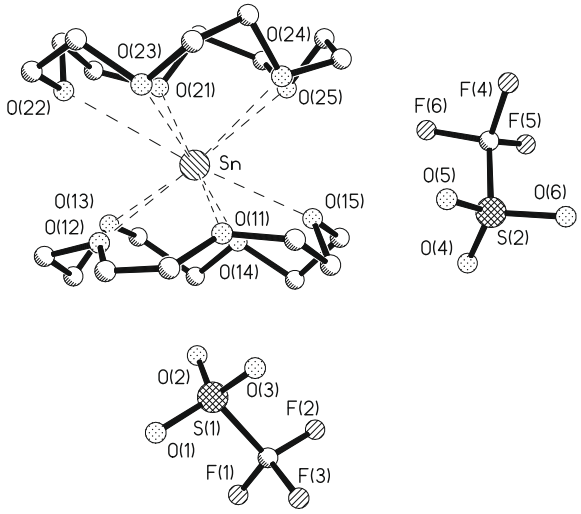

Fig. 2. Solid state structure of $[Sn([15]crown\text{-}5)_2][OTf]_2$, **2**$[OTf]_2$ – hydrogen atoms are omitted for clarity. Selected metrical parameters including distances (Å) and angles (°): Sn–O(11), 2.53(2); Sn–O(12), 2.59(1); Sn–O(13), 2.76(1); Sn–O(14), 2.75(1); Sn–O(15), 2.59(1); Sn–O(21), 2.83(1); Sn–O(22), 2.98(1); Sn–O(23), 2.87(1); Sn–O(24), 2.77(1); Sn–O(25), 2.83(1); centroid(O11–O15)-Sn–centroid(O21–O25), 175.3(1); plane(O11–O15)∠plane(O21–O25), 3.1(3).

solid-state ^{119}Sn NMR experiments reveal two very similar chemical shift manifolds with isotropic chemical shifts of −1721 and −1706 ppm that are consistent with the value predicted on the basis of the structure of **2**. It should be emphasized that the observation of these two similar but distinct signals is consistent with the presence of more than one crystalline form of the salt that was isolated, as had been suggested by the X-ray diffraction experiments and microanalytical data.

Finally, the treatment of tin(II) triflate with two equivalents of [12]crown-4 in THF provided the 2:1 crown ether complex [Sn([12]crown-4)$_2$][OTf]$_2$, **3**[OTf]$_2$ in excellent yield upon concentration. Recrystallization of the material from CH_2Cl_2 generated colorless crystals suitable for examination by single crystal X-ray diffraction. The salt crystallizes in the monoclinic space group $P2_1/c$ with one formula unit located in the asymmetric unit, the contents of which is illustrated in Fig. 3. The structure of **3**[OTf]$_2$ is best described as consisting of a bent-sandwich-like dicationic [Sn([12]crown-4)$_2$]$^{+2}$ fragment and two anionic triflate ions. Although it may appear as if the triflate group containing the oxygen atom labeled O(11) may be in close proximity to the open wedge of the cation, the Sn–O(11) distance of 3.119(4) Å is more than 0.5 Å longer than the Sn–O distance to the "anionic" OTf group in **1**[OTf] and it is longer than any of the Sn–O distances for triflate groups in the CSD. Furthermore, the S–O distances to S(1) are virtually equivalent to each other and to those of the "free" triflate ion containing S(2) thus suggesting that both of the fragments should described as ionic triflate species. Although the tin complex and the closest triflate ion may perhaps exist as some form of contact ion pair, the extreme length of the Sn–O interaction appears to render such a description implausible.

The dication **3** features four relatively short Sn–O bonds ranging from 2.474(3) to 2.495(3) Å (two from each of the crown ethers) and four substantially longer bonds ranging from 2.629(3) to 2.813(3) Å; the bent geometry of the sandwich is further evident from the angle between the O_4 planes in the two heterocycles 41.78(9)° and the 153.95(2)° angle at the tin atom between the O_4 centroid on each of the crown ethers. The bent arrangement of **3** contrasts sharply with the more conventional centrosymmetric sandwich observed for the germanium(II) analogue [Ge([12]-crown-4)$_2$]$^{+2}$ [3], as one might perhaps anticipate on the basis of the greater size of Sn^{II} versus Ge^{II}, and again may imply the presence of a stereochemically-active "lone pair" of electrons on the tin center. However, it should be noted that the *bis*([12]crown-4) complexes of potassium cations, which can not possibly have any non-bonding valence electrons, also exhibit structures in which the two macrocycles appear to be canted so as to expose a face of metal atom. In fact, the centroid-K-centroid angles for the complexes reported in the CSD range from roughly 155° to the perhaps anticipated 180° and the angles between the best-fit O_4 planes on the two rings range from 0° to almost 30° so the geometrical parameters of the complex do not appear to be an especially reliable indicator as to the presence of a stereochemically-active "lone-pair" of electrons on the encapsulated metal center. Given the foregoing, the reason(s) for the bent arrangement of **3** is not clear and the experimental observations we have obtained are not sufficient to allow for an unambiguous conclusion in that regard.

Finally, we wish to note that as in the case of the salts described above, resonances consistent with the presence of only a single type of crown ether and triflate ion are observed in the solution phase ^{1}H, ^{13}C and ^{19}F NMR spectra. Such behavior is consistent with the anticipated dynamic processes that are surely present both within the cationic fragment and between the component ions in solution. Once again, no signal is observed in the ^{119}Sn NMR spectrum in solution; however, the solid-state ^{119}Sn NMR spectrum features a single site with an isotropic chemical shift of −1405 ppm and a chemical shift anisotropy similar in magnitude to the other complexes.

2.2. Computational investigations

In light of the questions arising from the observations obtained from experimental investigations, we performed a series of density functional theory (DFT) calculations in order to assess whether the structural features that we have observed for the cationic fragments experimentally are consistent with the minimum energy structures that one would find in the gas phase or if the peculiarities of the structures are best attributable to the consequences of crystal packing effects. We also endeavored to gain insight into the nature of non-bonding electrons on the tin(II) atoms in such complexes through the analysis of the electron distribution in reasonable model compounds. The geometries of suitable model compounds for each of the cations were optimized in the absence of any constraints using the method described in Section 4. The optimized structures obtained for each of the model compounds containing [18]crown-6 ligands are presented in Fig. 4 and those containing the smaller crown ethers are depicted in Fig. 5; a summary of pertinent electronic and structural information is assembled in Table 1.

As illustrated in Fig. 4, the optimized structure of the model [Sn([18]crown-6)-OTf]$^{+1}$ cation is very similar to the structure of the mono-cationic fragment observed experimentally in the solid

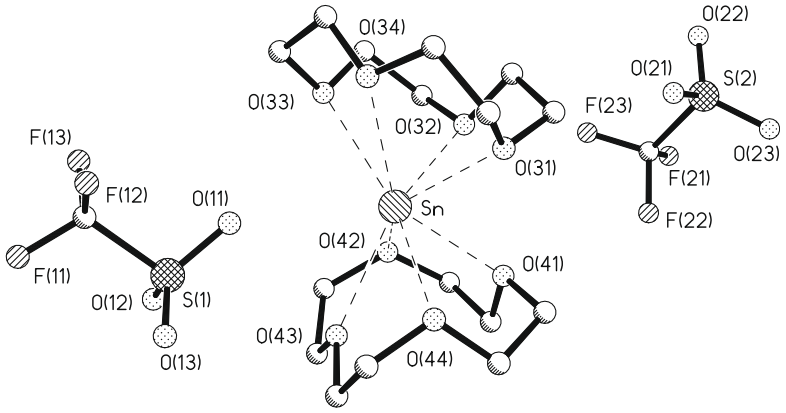

Fig. 3. Solid state structure of [Sn([12]crown-4)$_2$][OTf]$_2$, **3**[OTf]$_2$ – hydrogen atoms are omitted for clarity. Selected metrical parameters including distances (Å) and angles (°): Sn–O(11), 3.119(4); Sn–O(31), 2.476(4); Sn–O(32), 2.495(3); Sn–O(33), 2.741(4); Sn–O(34), 2.813(3); Sn–O(41), 2.475(4); Sn–O(42), 2.474(3); Sn–O(43), 2.629(3); Sn–O(44), 2.676(3); S(1)–O(11), 1.430(4); S(1)–O(12), 1.425(4); S(1)–O(13), 1.441(4); S(2)–O(21), 1.426(4); S(2)–O(22), 1.432(4); S(2)–O(23), 1.440(4); centroid(O(31)–O(34))–Sn-centroid(O(41)–O(44)), 153.95(2); plane(O(31)–O(34))∠plane(O(41)–O(44)), 41.78(9).

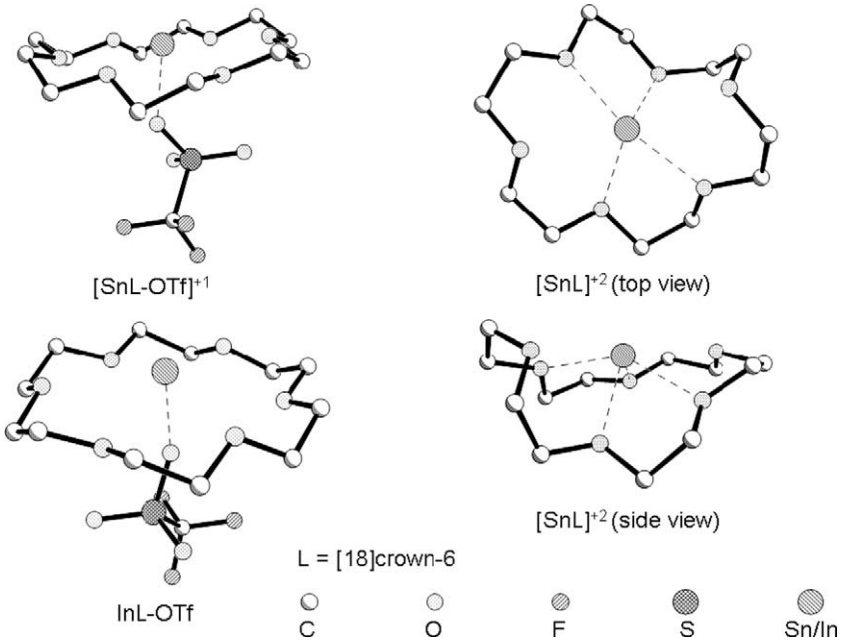

Fig. 4. DFT optimized structures for model compounds containing the [18]crown-6 ligand.

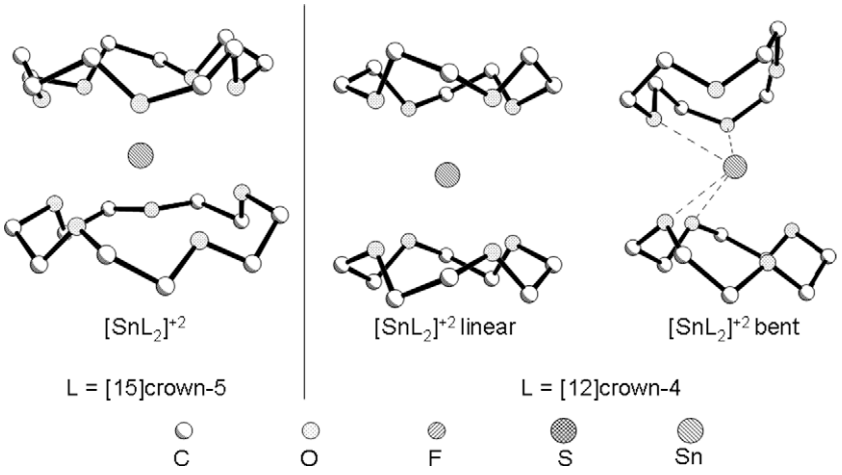

Fig. 5. DFT optimized structures for model compounds containing the [15]crown-5 and [12]crown-4 ligands.

Table 1
Selected calculated quantities from the DFT optimized structures of model compounds for tin and indium crown ether complexes; distances are reported in Å units.

	N_{imag}[a]	Q(M)[b]	LP(M)% 5s[c]	WBI[d] (M–O_{ring}) range	WBI[d] (M–OTf)	WBI[d] (M) total	R(M–O_{ring}) range	r(M-OTf)
L = [18]crown-6								
$[SnL]^{+2}$	0	1.50	97.49	0.1132–0.1729	–	0.9928	2.426–2.636	–
$[SnL–OTf]^{+1}$	0	1.44	95.96	0.1007–0.1117	0.2883	1.0899	2.692–2.760	2.125
InL–OTf	0	0.74	95.72	0.0446–0.0530	0.1136	0.6065	2.805–2.962	2.253
L = [15]crown-5								
$[SnL_2]^{+2}$	0	1.36	99.88	0.0857–0.1193	–	1.2268	2.620–2.994	–
L = [12]crown-4								
$[SnL_2]^{+2}$ bent	0	1.43	98.26	0.0967–0.1396	–	1.1398	2.484–2.767	–
$[SnL_2]^{+2}$ linear	1[e]	1.42	100.00	0.1181–0.1185	–	1.1535	2.630–2.634	–

[a] Number of imaginary frequencies in the Hessian matrix.
[b] NBO charge on the metal atom.
[c] NBO percentage of 5s character in the "lone pair" orbital on the metal atom.
[d] NBO Wiberg Bond Index for the bonds indicated.
[e] This transition state is less stable than the bent geometry by ca. 17 kJ/mol; the imaginary frequency has a value of $-29.1\ cm^{-1}$.

state with two notable deviations: (1) the tin atom is predicted to reside in the center of the crown ether roughly 0.2 Å above the O_6 centroid opposite the triflate fragment while the tin atom in the crystal structure is located off center and toward one edge of the

macrocyclic ligand; and, (2) the calculated Sn–O distance of 2.125 Å to the triflate ligand is significantly shorter than the 2.282(9) Å observed experimentally. In contrast, the triflate-free dication model $[Sn([18]crown-6)]^{+2}$ features a very distorted crown ether that does not resemble any of the structures that have ever been observed experimentally. Overall, these observations suggest that although the mono-cationic model $[Sn([18]crown-6)-OTf]^{+1}$ is certainly more appropriate than the dicationic alternative, the interaction of the anionic triflate with the mono-cationic fragment in the real compound is clearly sufficient to perturb the system noticeably.

As for the analysis of the electronic structure of the [18]crown-6 model systems, we wish to note that the Wiberg Bond Index of around 0.29 for the Sn–OTf bond is significantly larger than the corresponding value of 0.11 found for the isoelectronic indium(I) model, as one would anticipate given the higher electronegativity and charge of Sn^{II} versus In^{I}; this observation is also consistent with the interpretation of $[Sn([18]crown-6)-OTf]^{+1}$ as being bound comparatively tightly. Nevertheless, we wish to emphasize that in spite of the significant interaction between the tin atom and the triflate group, the non-bonding pair of electrons on the tin atom remains almost exclusively (ca. 96%) 5s in character, as expected on the basis of the results of the Mössbauer experiments performed on the related halide cations.

The optimized structure of the model $[Sn([15]crown-5)_2]^{+2}$, as depicted in Fig. 5, is completely consistent with those observed in the solid state both in this work and in the previous report and requires no additional comment. As one would predict on the basis of the roughly centrosymmetric coordination environment about the tin atom, the non-bonding valence electrons on tin are predicted to reside in an orbital that is essentially exclusively of 5s character. Attempted geometry optimizations on "bent sandwich" models of $[Sn([15]crown-5)_2]^{+2}$ invariably resulted in the same nearly centrosymmetric structure illustrated in Fig. 5.

For the [12]crown-4 complexes, the geometry optimizations provided two different possible dicationic $[Sn([12]crown-4)_2]^{+2}$ model compounds illustrated in Fig. 5; one having a roughly centrosymmetric arrangement of crown ether ligands (labeled "linear" in the figure) and one having a "bent" geometry more similar to the structure observed experimentally. Frequency analyses on the two optimized structures reveal that whereas the bent structure is a true minimum, the linear structure exhibits one imaginary frequency (albeit of only $-29.1\ cm^{-1}$) and is approximately 17 kJ/mol less stable than the bent model. Thus it is clear that the adoption of a bent geometry is not simply an effect of crystal packing but is an integral feature of this complex. Furthermore, it should be noted that the optimized model structure matches the experimental one almost perfectly, as illustrated in Fig. 6, which suggests that the apparent interaction between the sandwich complex and the triflate anion does not actually affect the structure of the dication in a significant manner. Regardless of the geometry adopted by the sandwich complex, the non-bonding electrons are again found to reside in an orbital that is more than 98% 5s character.

3. Conclusions

The treatment of $Sn^{II}OTf_2$ with crown ethers produces coordination complexes of Sn^{II} featuring dramatically different structural features depending on the size of the ligand. The largest ligand, [18]crown-6 is sufficiently large enough to encircle the metal and produces a mono-cationic salt of the form [Sn([18]crown-6)-OTf][OTf], the cation of which appears to feature a stereochemically-active "lone pair" of electrons. A single [15]crown-5 macrocycle is too small to encircle the Sn^{II} center and instead a centrosymmetric sandwich-like dicationic complex is generated of the form $[Sn([15]crown-5)_2][OTf]_2$ that appears to have a non-bonding pair of electrons that is stereochemically-inactive. Finally, the smallest of the macrocycles, [12]crown-4, also produces a 2:1 complex of the form $[Sn([12]crown-4)_2][OTf]_2$, however the structure of the dication is bent and again appears to be consistent with a stereochemically-active pair of non-bonding electrons. Computational investigations predict the observed structures quite well and suggest that the non-bonding valence electrons on tin are always almost exclusively 5s in character regardless of the gross structural features of the complex; the small magnitudes observed for the chemical shielding anisotropies of the Sn^{II} centers in each of the solid-state ^{119}Sn NMR experiments (see the Supporting Information) are consistent with this interpretation.

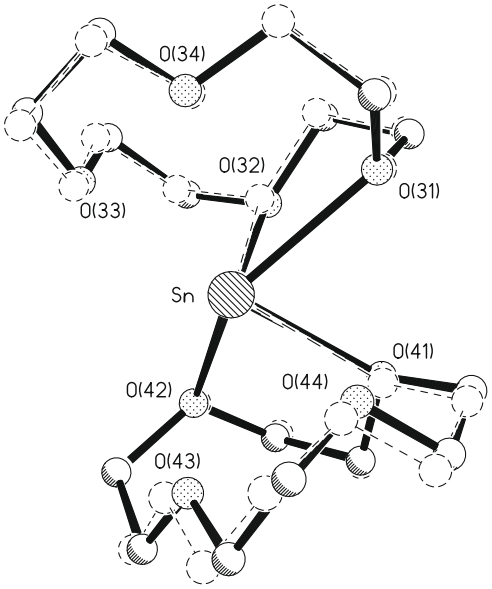

Fig. 6. Overlay of the DFT optimized structure (dotted) and the experimental structure (solid) for the $[Sn([12]crown-4)_2]^{+2}$ complex.

As a final observation, we wish to note that in stark contrast to the related In^{I} species, none of the Sn^{II} complexes appear to undergo insertion chemistry into the C–Cl bonds of chlorocarbon solvents. In fact, as indicated above, several of the complexes are actually recrystallized from such solvents.

4. Experimental

4.1. General methods

All work was carried out using standard inert-atmosphere techniques. All reagents and solvents were obtained from Aldrich or Strem and were used without further purification. Solvents were dried on a series of Grubbs'-type columns and were degassed prior to use [20]. C_6D_6 and CD_2Cl_2 were distilled over CaH_2 and then stored over 4 Å molecular sieves. Unless otherwise noted in the text, NMR spectra were recorded at room temperature on either a Bruker DPX 300 MHz spectrometer or a DRX 500 MHz spectrometer. Chemical shifts are reported in ppm, relative to external standards ($SiMe_4$ for ^1H and ^{13}C; $CFCl_3$ for ^{19}F; $SnMe_4$ for ^{119}Sn). Details of the solid-state NMR experiments are presented in the supporting information. Melting points were obtained using an Electrothermal® melting point apparatus on samples sealed in glass capillaries under dry nitrogen. Elemental analysis was performed at Guelph Chemical Laboratories, Guelph, Ontario, Canada.

4.2. Synthesis of [SnOTf([18]crown-6)][OTf], **1**[OTf]

A solution of [18]crown-6 (0.634 g, 2.40 mmol) in toluene was added to a solution of $Sn(OTf)_2$ (1.00 g, 2.64 mmol) in toluene. The resultant colorless solution was left to stir for 24 h. Slow evaporation of the solvent produced a colorless crystalline material which was identified as [SnOTf([18]crown-6)][OTf] (1.53 g, 93%). Please note that while this compound was reported in the supporting information of our preliminary communication about Ge^{II} complexes [3], the data are included here for completeness.^{1}H NMR (CD_2Cl_2): 3.12 (s, CH_2)^{13}C NMR (CD_2Cl_2): 70.6 (s, CH_2)^{19}F NMR (CD_2Cl_2): −78.4^{119}Sn NMR (solid state, isotropic chemical shift): −1578(2)D.P.: ca. 210 °C*Anal.* Calc. for $C_{14}H_{24}F_6SnO_{12}S_2$: C, 24.69; H, 3.55; O, 28.18. Found: C, 24.22; H, 3.19; O, 27.70%.

4.3. Synthesis of [Sn([15]crown-5)$_2$][OTf]$_2$, **2**[OTf]$_2$

A solution of [15]crown-5 (0.20 mL, 0.214 g, 0.972 mmol) in THF was added to a solution of $Sn(OTf)_2$ (0.200 g, 0.480 mmol) in THF. The resultant colorless solution was left for stirring for 2 h after which all volatile components were removed under reduced pressure. The remaining colorless solid product was washed with pentane (5 mL) to yield a colorless solid characterized as [Sn([15]crown-5)$_2$][OTf]$_2$ (0.401 g, 0.468 mmol, 97% – please see below). Single crystals adequate for X-ray diffraction studies were obtained through the evaporation of a CH_2Cl_2 solution of this solid; the crystalline material was identified as [Sn([15]crown-5)$_2$][OTf]$_2$ – please note that we have also obtained crystals obtained under almost identical conditions that feature a different unit cell with composition [Sn([15]crown-5)$_2$][OTf]$_2$·$x$$CH_2Cl_2$.^{1}H NMR ($CD_2Cl_2$): 3.85 (s, CH_2)^{13}C NMR (CD_2Cl_2): 69.4 (s, CH_2)^{19}F NMR (CD_2Cl_2): −79.3^{119}Sn NMR (solid state, isotropic chemical shift): −1721(2) and −1706(2)M.P.: 159–165 °C

We have not yet been able to obtain reliable microanalytical data for this salt. Our crystallographic investigations reveal that the salt **2**[OTf]$_2$ can crystallize in at least two different forms, each having different unit cells, one of which features solvent of crystallization (and partial occupancy of the void occupied by the solvent is also possible), thus the composition of even the crystalline portion of the solid obtained deviates from the anticipated elemental percentages calculated for $C_{22}H_{40}F_6SnO_{16}S_2$: C, 30.82; H, 4.70; O, 29.86.

4.4. Synthesis of [Sn([12]crown-4)$_2$][OTf]$_2$, **3**[OTf]$_2$

A solution of [12]crown-4 (0.15 mL, 0.166 g, 0.943 mmol) in THF was added to a solution of $Sn(OTf)_2$ (0.200 g, 0.479 mmol) in THF. The resultant colorless solution was left for stirring for 2 h after which all volatile components were removed under reduced pressure. The remaining white solid product was washed with pentane (5 mL) and dried under reduced pressure to yield a colorless solid characterized as [Sn([12]crown-4)$_2$][OTf]$_2$ (0.355 g, 0.465 mmol, 96%). Single crystals suitable for X-ray diffraction studies were obtained through the evaporation of a CH_2Cl_2 solution of this solid; the crystalline material was identified as [Sn([12]crown-4)$_2$][OTf]$_2$ (0.125 g, 0.162 mmol, 34% crystalline yield).^{1}H NMR (CD_2Cl_2): 3.83 (s, CH_2)^{13}C NMR (CD_2Cl_2): 69.5 (s, CH_2)^{19}F NMR (CD_2Cl_2): −79.4^{119}Sn NMR (solid state, isotropic chemical shift): −1405(2)M.P.: 149–152 °C*Anal.* Calc. for $C_{18}H_{32}F_6SnO_{14}S_2$: C, 28.10; H, 4.19; O, 29.12. Found: C, 28.48; H, 4.46; O, 29.60%.

4.5. Crystallography

The subject crystals were covered in Nujol® or Paratone-N®, mounted on a goniometer head and rapidly placed in the dry N_2 cold-stream of the low-temperature apparatus (Kryoflex) attached to the diffractometer. The data were collected using the SMART [21] software on a Bruker APEX CCD diffractometer using a graphite monochromator with Mo Kα radiation (λ = 0.71073 Å). A hemisphere of data was collected for each crystal using a counting times ranging from 10 to 30 s per frame at −100 °C. Details of crystal

Table 2
Summary of crystallographic data for the compounds in this work.

Compound	[SnOTf([18]crown-6)][OTf]	[Sn([15]crown-5)$_2$][OTf]$_2$	[Sn([12]crown-4)$_2$][OTf]$_2$
Compound number	**1**[OTf]	**2**[OTf]$_2$	**3**[OTf]$_2$
CCD number	722429	749124	749123
Empirical formula	$C_{14}H_{24}F_6O_{12}S_2Sn$	$C_{22}H_{40}F_6O_{16}S_2Sn$	$C_{18}H_{32}F_6O_{14}S_2Sn$
Formula weight	681.14	857.35	769.25
Temperature (K)	173(2)	173(2)	173(2)
Wavelength (Å)	0.71073	0.71073	0.71073
Crystal system	Triclinic	Monoclinic	Monoclinic
Space group	$P\bar{1}$	$P2_1/c$	$P2_1/c$
a (Å)	9.837(2)	12.6206(14)	11.7148(10)
b (Å)	9.896(2)	13.8047(16)	12.5654(11)
c (Å)	14.094(3)	20.390(2)	19.2307(17)
α (°)	71.430(3)	90	90
β (°)	74.194(3)	107.9810(10)	95.0820(10)
γ (°)	71.627(3)	90	90
Volume (Å^3)	1211.5(5)	3378.9(7)	2819.7(4)
Z	2	4	4
Absorbed coefficient (mm^{-1})	1.329	0.980	1.158
F(0 0 0)	680	1744	1552
Color	Colorless	Colorless	Colorless
Crystal size (mm^3)	0.10 × 0.10 × 0.10	0.40 × 0.20 × 0.20	0.30 × 0.20 × 0.15
θ Range for data collection (°)	1.55–25.00	1.70–27.50	1.75–27.50
Data/restraints/parameters	4240/0/317	7669/0/424	6373/0/370
Goodness-of-fit F^2, S[b] (all data)	1.043	1.099	1.089
Final R indices [$I > 2\sigma(I)$][a]	0.0832	0.1412	0.0457
wR_2 indices (all data) [a]	0.1261	0.4130	0.1455
Largest differences in peak and hole (e Å^{-3})	1.319 and −0.874	5.845 and −1.210	1.173 and −0.680

[a] $R_1(F) = \Sigma(|F_o| - |F_c|)/\Sigma|F_o|\}$ for reflections with $F_o > 4(\sigma(F_o))$. $wR_2(F^2) = \{\Sigma w(|F_o|^2 - |F_c|^2)^2/\Sigma w(|F_o|^2)^2\}^{1/2}$, where w is the weight given each reflection.
[b] $S = [\Sigma w(|F_o|^2 - |F_c|^2)^2]/(n - p)^{1/2}$, where n is the number of reflections and p is the number of parameters used.

data, data collection and structure refinement are listed in Table 2. Data reduction was performed using the SAINT-PLUS [22] software and the data were corrected for absorption using SADABS [23]. The structure was solved by direct methods using SIR97 [24] and refined by full-matrix least-squares on F^2 with anisotropic displacement parameters for the non-disordered heavy atoms using SHELXL-97 [25] and the WINGX [26] software package and thermal ellipsoid plots were produced using SHELXTL [27]. The space group assignments and structural solutions were evaluated using PLATON [28]. Powder X-ray diffraction (pXRD) experiments that confirm that the bulk materials are consistent with the single crystal structures were performed with a Bruker D8 Discover diffractometer equipped with a Hi-Star area detector using Cu Kα radiation (λ = 1.54186 Å). It must be noted that for [Sn([15]crown-5)$_2$][OTf]$_2$, we were never able to obtain crystals of high quality: the crystals are often non-merohedrally twinned with a vast number of different orientations and sometimes crystallize in a larger apparently orthorhombic unit cell (18.688(4) Å × 26.249(6) Å × 35.345(8)) featuring partial inclusion of CH_2Cl_2 solvent molecules, even from crystallization conditions identical to those that produced the monoclinic crystals reported above. Regardless, the data for the monoclinic crystal, while of low quality (R_{int} = 0.1088), are clearly sufficient to establish the connectivity of the molecule without any ambiguity.

Thermal ellipsoid plots of each of the structures are depicted in the supporting information. The supplementary crystallographic data for this paper has been deposited in the Cambridge Crystallographic Data Centre. These data can be obtained free of charge from The Cambridge Crystallographic Data Centre via www.ccdc.cam.ac.uk/data_request/cif using the CCDC numbers in Table 2.

4.6. Theoretical calculations

All of the computational investigations were performed on the node of the Shared Hierarchical Academic Research Computing Network (SHARCNET) facilities located at the University of Windsor (tiger.sharcnet.ca) using the GAUSSIAN03 suite of programs [29]. Geometry optimizations were conducted using density functional theory (DFT), specifically implementing the B3PW91 method [containing Becke's three-parameter hybrid functional for exchange (B3, including ca. 20% Hartree–Fock exchange) [30] combined with the generalized gradient approximation for correlation of Perdew and Wang (PW91) [31]] in conjunction with Stuttgart/Dresden (SDD) relativistic effective core pseudopotential and basis set for Sn and In [32] and the 6-31G(d) basis set for all other atoms. The geometry optimizations were not subjected to any symmetry restrictions and each stationary point was confirmed to be a minimum having zero imaginary vibrational frequencies unless otherwise indicated. Population analyses were conducted using the Natural Bond Orbital (NBO) [33] implementation included with the GAUSSIAN03 package.

Acknowledgment

The funding that has enabled this work has been provided by the Natural Sciences and Engineering Research Council of Canada (NSERC), the Canada Foundation for Innovation, the Ontario Innovation Trust and the Ontario Research and Development Challenge Fund (University of Windsor Centre for Catalysis and Materials Research), and the Ontario Ministry of Research and Innovation (Early Researcher Award). This work was made possible by the facilities of the Shared Hierarchical Academic Research Computing Network (SHARCNET:www.sharcnet.ca) and Compute/Calcul Canada. We thank Dr. Matthew Revington for assistance with the collection of NMR spectra. We thank NSERC and the Government of Ontario for scholarship support. Finally, we thank a referee for some useful suggestions.

Appendix A. Supplementary material

Supplementary data associated with this article can be found, in the online version, at doi:10.1016/j.jorganchem.2009.12.023.

References

[1] G.W. Gokel (Ed.), Comprehensive Supramolecular Chemistry, in: J.-M. Lehn, J.L. Atwood, J.E.D. Davies, D.D. MacNicol, F. Vogtle (Series Eds.), Molecular Recognition: Receptors for Cationic Guests, vol. 1, Elsevier Science Ltd., Oxford, 1996.
[2] D.A. Rogers, C.B. Bauer, G.W. Gokel (Eds.), Structural Chemistry of Metal-Crown Ether and Polyethylene Glycol Complexes Excluding Groups 1 and 2, Comprehensive Supramolecular Chemistry: Molecular Recognition: Receptors for Cationic Guests, vol. 1, Elsevier Science Ltd., Oxford, 1996, p. 315.
[3] P.A. Rupar, R. Bandyopadhyay, B.F.T. Cooper, M.R. Stinchcombe, P.J. Ragogna, C.L.B. Macdonald, K.M. Baines, Angew. Chem., Int. Ed. 48 (2009) 5155.
[4] T. Muller, Angew. Chem., Int. Ed. 48 (2009) 3740.
[5] F. Cheng, A.L. Hector, W. Levason, G. Reid, M. Webster, W.J. Zhang, Angew. Chem., Int. Ed. 48 (2009) 5152.
[6] P.A. Rupar, V.N. Staroverov, K.M. Baines, Science 322 (2008) 1360.
[7] C.L.B. Macdonald, A.M. Corrente, C.G. Andrews, A. Taylor, B.D. Ellis, Chem. Commun. (2004) 250.
[8] C.G. Andrews, C.L.B. Macdonald, Angew. Chem., Int. Ed. 44 (2005) 7453.
[9] B.F.T. Cooper, C.G. Andrews, C.L.B. Macdonald, J. Organomet. Chem. 692 (2007) 2843.
[10] B.F.T. Cooper, C.L.B. Macdonald, J. Organomet. Chem. 693 (2008) 1707.
[11] B.F.T. Cooper, C.L.B. Macdonald, Main Group Chem. (2009) in press.
[12] C.L.B. Macdonald, B.D. Ellis, Low oxidation state main group chemistry, in: R.B. King (Ed.), Encyclopedia of Inorganic Chemistry, John Wiley and Sons Ltd., 2005.
[13] M.G.B. Drew, D.G. Nicholson, J. Chem. Soc., Dalton Trans. (1986) 1543.
[14] E. Hough, D.G. Nicholson, A.K. Vasudevan, J. Chem. Soc., Dalton Trans. (1989) 2155.
[15] R.H. Herber, A.E. Smelkinson, Inorg. Chem. 17 (1978) 1023.
[16] R.H. Herber, G. Carrasquillo, Inorg. Chem. 20 (1981) 3693.
[17] M. Wolff, T. Harmening, R. Pottgen, C. Feldmann, Inorg. Chem. 48 (2009) 3153.
[18] C.E. Housecroft, A.G. Sharpe, Inorganic Chemistry, third ed., Pearson Education Ltd., Harlow, 2008.
[19] F.H. Allen, Acta Crystallogr., Sect. B: Struct. Sci. 58 (2002) 380.
[20] A.B. Pangborn, M.A. Giardello, R.H. Grubbs, R.K. Rosen, F.J. Timmers, Organometallics 15 (1996) 1518.
[21] SMART, Bruker AXS Inc.: Madison, WI, 2001.
[22] SAINTPLUS, Bruker AXS Inc.: Madison, WI, 2001.
[23] SADABS, Bruker AXS Inc.: Madison, WI, 2001.
[24] A. Altomare, M.C. Burla, M. Camalli, G.L. Cascarano, C. Giacovazzo, A. Guagliardi, A.G.G. Moliterni, G. Polidori, R. Spagna, J. Appl. Crystallogr. 32 (1999) 115.
[25] G.M. Sheldrick, SHELXL-97, Universitat Gottingen, Gottingen, 1997.
[26] L.J. Farrugia, J. Appl. Crystallogr. 32 (1999) 837.
[27] G.M. Sheldrick, SHELXTL, Bruker AXS Inc.: Madison, WI, 2001.
[28] A.L. Spek, J. Appl. Crystallogr. 36 (2003) 7.
[29] M.J. Frisch, G.W. Trucks, H.B. Schlegel, G.E. Scuseria, M.A. Robb, J.R. Cheeseman, J.A. Montgomery, T. Vreven, K.N. Kudin, J.C. Burant, J.M. Millam, S.S. Iyengar, J. Tomasi, V. Barone, B. Mennucci, M. Cossi, G. Scalmani, N. Rega, G.A. Petersson, H. Nakatsuji, M. Hada, M. Ehara, K. Toyota, R. Fukuda, J. Hasegawa, M. Ishida, T. Nakajima, Y. Honda, O. Kitao, H. Nakai, M. Klene, X. Li, J.E. Knox, H.P. Hratchian, J.B. Cross, V. Bakken, C. Adamo, J. Jaramillo, R. Gomperts, R.E. Stratmann, O. Yazyev, A.J. Austin, R. Cammi, C. Pomelli, J.W. Ochterski, P.Y. Ayala, K. Morokuma, G.A. Voth, P. Salvador, J.J. Dannenberg, V.G. Zakrzewski, S. Dapprich, A.D. Daniels, M.C. Strain, O. Farkas, D.K. Malick, A.D. Rabuck, K. Raghavachari, J.B. Foresman, J.V. Ortiz, Q. Cui, A.G. Baboul, S. Clifford, J. Cioslowski, B.B. Stefanov, G. Liu, A. Liashenko, P. Piskorz, I. Komaromi, R.L. Martin, D.J. Fox, T. Keith, A. Laham, C.Y. Peng, A. Nanayakkara, M. Challacombe, P.M.W. Gill, B. Johnson, W. Chen, M.W. Wong, C. Gonzalez, J.A. Pople, GAUSSIAN03, Revision D.01, 2003.
[30] A.D. Becke, J. Chem. Phys. 98 (1993) 5648.
[31] J.P. Perdew, Y. Wang, Phys. Rev. B 45 (1992) 13244.
[32] A. Bergner, M. Dolg, W. Kuchle, H. Stoll, H. Preuss, Mol. Phys. 80 (1993) 1431.
[33] A.E. Reed, L.A. Curtiss, F. Weinhold, Chem. Rev. 88 (1988) 899.